Conditions for synchronization in Josephson-junction arrays

A. A. Chernikov and G. Schmidt
Stevens Institute of Technology, Hoboken, New Jersey 07030
(Received 6 April 1995)

An effective perturbation theoretical method has been developed to study the dynamics of Josephson-junction series arrays. It is shown that the inclusion of junction capacitances, which is often ignored, has a significant impact on synchronization. Comparison of analytic with computational results over a wide range of parameters shows excellent agreement.

PACS number(s): 05.45.+b

INTRODUCTION

Josephson junctions are known to produce very high frequency oscillations and can be used to generate submillimeter range radiation [1–3]. The difficulty is the low power output of individual junctions. This could be remedied by the use of many synchronized coupled junctions. Figure 1 shows a sketch of N junctions in series, fed by a constant dc current source and shunted by a load of impedance Z. The junctions have an internal resistance, as well as a capacitance.

In normalized units this circuit is described by

$$\beta\ddot{\varphi}_k+\dot{\varphi}_k+\sin(\varphi_k)+I_L=I \ , \tag{1}$$

where φ_k represents the phase difference of the wave function across the kth junction, β corresponds to the capacitance of the junction, I_L is the load current. Without the load, the system can be visualized as a point particle of mass β sliding down an incline of steepness I, sinusoidally modulated, with air resistance represented by $\dot{\varphi}_k$.

To arrive at the normalized units one rescales time $2eR_JI_ct/\hbar\to t$, where R_J is the Ohmic resistance of a junction and I_c is the critical current, the current $I/I_c\to I$, and $\beta=2eR_J^2I_cC_J/\hbar$ with C_J the junction capacitance.

The load current depends on the voltage across the array, proportional to $\sum_j\dot{\varphi}_j$. For instance, for a load made up of an inductance, capacitance, and resistance in series one writes in normalized units

$$L\dot{I}_L+RI_L+(1/C)\int I_L dt=(1/N)\sum_j\dot{\varphi}_j \ . \tag{2}$$

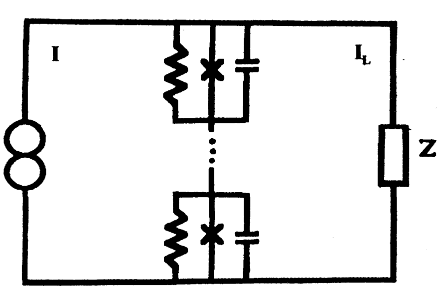

FIG. 1. Sketch of the circuit investigated. Constant current I feeds the system, the junctions form one-dimensional array with resistive and capacitive characteristics, coupled to an impedance Z.

These equations are clearly nonlinear and no analytic solutions are available.

Recently several authors [4–9] analytically investigated a simplified version of these equations. The load capacitance has been ignored ($\beta=0$) and the coupling to the load (I_L) has been assumed to be small, so perturbation theory could be used. Under these conditions it was shown that for a purely resistive load the equations are integrable [7]. The present authors have shown [9] that if a slight difference between the individual junction parameters is introduced, integrability fails and chaotic behavior follows. Quite recently Wiesenfeld and Swift [8] analytically studied the simplified equations of identical junctions with $\beta=0$ in the weak coupling limit, and found that the synchronous solutions are stable if the load is predominantly inductive and unstable if it is capacitive. Similar results have been obtained earlier by Jain *et al.* using a different approach [10]. The dividing line is at resonance when the Josephson-junction frequency equals the resonant frequency of the load $(LC)^{-2}$.

Computed solutions of the equations show, however, that the junction capacitance has a significant effect on the stability of synchronized solutions, even for $\beta\ll 1$. Here a powerful perturbation theoretical method is developed where β, as well as the coupling strength, can be arbitrarily large, and excellent agreement is found with computer generated solutions.

CAPACITIVE LOAD COMPUTATION

First we rewrite Eqs. (1) and (2), by dividing (1) by I, and rescaling time $It\to t$ and $I\beta\to\beta$, to get

$$\beta\ddot{\varphi}_k+\dot{\varphi}_k+b\sin(\varphi_k)+J=1 \ , \tag{3}$$

$$\mu_1\dot{J}+\mu_2 J+\int J\,dt=\alpha\sum_j\dot{\varphi}_j \ , \tag{4}$$

where $J=I_L/I$, $b=I^{-1}$, $\mu_1=LCI^2$, $\mu_2=RCI$, $\alpha=IC/N$. For a purely capacitive load, $\mu_1=\mu_2=0$, and these equa-

1063-651X/95/52(4)/3415(5)/$06.00 ©1995 The American Physical Society

tions reduce to

$$\beta\ddot{\varphi}_k+\dot{\varphi}_k+b\sin(\varphi_k)+\alpha\sum_j\ddot{\varphi}_j=1 . \tag{5}$$

In order to study the linear stability of the synchronous solutions, one can expand $\varphi_k=\varphi_0+\delta\varphi_k$, where φ_0 satisfies the

$$\beta\ddot{\varphi}_0+\dot{\varphi}_0+b\sin(\varphi_0)+N\alpha\varphi_0=1 \tag{6}$$

equation, while for $\delta\varphi_k$ one has

$$\beta\delta\ddot{\varphi}_k+\delta\dot{\varphi}_k+b\cos(\varphi_0)\delta\varphi_k+\alpha\sum_j\ddot{\varphi}_j=0 . \tag{7}$$

Subtracting the kth from lth equation gives [5]

$$\beta\ddot{\Delta}_{l,k}+\dot{\Delta}_{l,k}+b\cos(\varphi_0)\Delta_{l,k}=0 , \tag{8}$$

where $\Delta_{l,k}=\delta\varphi_1-\delta\varphi_k$. Linear stability implies that $\Delta_{l,k}$ asymptotically tends to zero. One solves Eq. (6) on the computer, for given parameters β, b, and $N\alpha$, and the computed function φ_0 in Eq. (8) to determine the long time behavior of $\Delta_{l,k}$. Since $I>1$, the parameter b is always less than one ($|I|<1$ is in the hysteresis regime).

Figure 2 shows the β-$N\alpha$ curve constructed for $b=0.5$, $b=0.25$, and $b=0.1$. Two important conclusions follow.

(i) The three curves practically coincide, and the differences are within the width of the line.

(ii) While for $\beta=0$ the synchronous state is always linearly unstable as expected [8], for large coupling even the addition of small junction capacitance can stabilize the state. For example, when $N\alpha=10$, $\beta>0.1$ gives stability. When $\beta>1$ stability persists for any value of the coupling.

The first condition suggests an analytic method. Since the solution is essentially independent of b, one can carry out an analytic calculation based on a small b expansion. Since b is the coefficient of the only nonlinear term, the expansion can be reduced to the solution of set of linear equations.

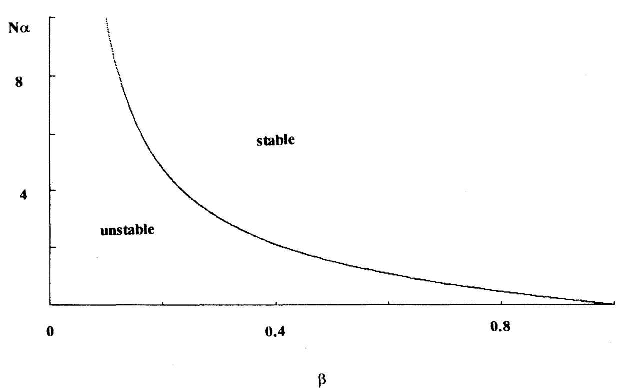

FIG. 2. Computed dividing line between stable and unstable regions in β-αN parameter space of capacitive loaded arrays.

CAPACITIVE LOAD ANALYSIS

To the lowest order in the expansion in b, Eq. (5) gives $\varphi_k=t+\theta_k$. The first order terms are

$$\beta\ddot{\varphi}_k^{(1)}+\dot{\varphi}_k^{(1)}+\alpha\sum_j\ddot{\varphi}_j^{(1)}+b\sin(t+\theta_k)=0 , \tag{9}$$

giving second order linear inhomogeneous equations, with the oscillating solutions

$$\varphi_k^{(1)}=A_k\sin(t)+B_k\cos(t) , \tag{10}$$

where coefficients are determined from

$$\beta A_k+B_k+\alpha\sum_j A_j-b\cos\theta_k=0 , \tag{11}$$

$$A_k-\beta B_k-\alpha\sum_j B_j+b\sin\theta_k=0 . \tag{12}$$

Summation over all junctions gives

$$(\beta+N\alpha)\sum_j A_j+\sum_j B_j-b\sum_j\cos\theta_j=0 , \tag{13}$$

$$-(\beta+N\alpha)\sum_j B_j+\sum_j A_j+b\sum_j\sin\theta_j=0 , \tag{14}$$

with the solution

$$\sum_j A_j=b[1+(\beta+N\alpha)^2]^{-1}\left[(\beta+N\alpha)\sum_j\cos\theta_j-\sum_j\sin\theta_j\right] , \tag{15}$$

$$\sum_j B_j=b[1+(\beta+N\alpha)^2]^{-1}\left[(\beta+N\alpha)\sum_j\sin\theta_j+\sum_j\cos\theta_j\right] . \tag{16}$$

Substituting these expressions into Eqs. (11) and (12) gives

$$A_k=b(1+\beta^2)^{-1}(-\sin\theta_k+\beta\cos\theta_k) +b\alpha(1+\beta^2)^{-1}[1+(\beta+\alpha N)^2]^{-1} \times\left[(1-\beta^2-\beta\alpha N)\sum_j\cos\theta_j+(2\beta+\alpha N)\sum_j\sin\theta_j\right] , \tag{17}$$

$$B_k=b(1+\beta^2)^{-1}(\cos\theta_k+\beta\sin\theta_k) +b\alpha(1+\beta^2)^{-1}[1+(\beta+\alpha N)^2]^{-1} \times\left[(1-\beta^2-\beta\alpha N)\sum_j\sin\theta_j-(2\beta+\alpha N)\sum_j\cos\theta_j\right] . \tag{18}$$

The second order expansion of Eq. (5) gives

$$\beta\ddot{\varphi}_k^{(2)}+\dot{\varphi}_k^{(2)}+\alpha\sum_j\varphi_j^{(2)}+b\cos(t+\theta_k)\varphi_k^{(1)}=0 , \tag{19}$$

where $\varphi_k^{(1)}$ is given by Eqs. (10), (17), and (18). The driving term in Eq. (19) contains second harmonics, as well as time independent terms. Synchronization, as well as desynchronization, is due to long time behavior, compared to the oscillation time scale. It is useful therefore to consider the time averaged term

$$\langle b\cos(t+\theta_k)\varphi_k^{(1)}\rangle=(b/2)(B_k\cos\theta_k-A_k\sin\theta_k)$$

$$=(b^2/2)(1+\beta^2)^{-1}+\alpha(b^2/2)(1+\beta^2)^{-1}[1+(\beta+\alpha N)^2]^{-1}\left[(1-\beta^2-\beta\alpha N)\sum_j\sin(\theta_j-\theta_k)-(2\beta+\alpha N)\sum_j\cos(\theta_j-\theta_k)\right]. \quad (20)$$

So from Eqs. (19) and (20)

$$\varphi_k^{(2)}\sim-\langle b\cos(t+\theta_k)\varphi_k^{(1)}\rangle t+(\text{second harmonic terms}) . \quad (21)$$

One may think of the φ_k's as points moving on the unit circle. To lowest order they move with unit phase velocity separated by angles $\theta_j-\theta_k$. The first order solutions of Eq. (10) add oscillatory motion, while to second order, second harmonics of the oscillatory motion appear as well as a change in the time average velocity. The first term in Eq. (20) describes a slowing of all points to $1-(b^2/2)(1+\beta^2)^{-1}$. The other two terms arise from the interaction of different points. Synchronization (or desynchronization) is described by the first of these terms. When $\beta=0$ the angle differences $\theta_j-\theta_k$ grow toward a splay state. Past a threshold value of β the angle differences contract until synchronization is achieved. This threshold is given by the equation

$$1-\beta^2-\beta\alpha N=0 . \quad (22)$$

This is an excellent fit to the curve in Fig. 2. Finally the last term in Eq. (20) describes the increase of phase velocities of points as they approach each other to the synchronous state, or the decrease of velocities as a splay state is approached.

ANALYSIS OF THE SYSTEM WITH A *RLC* LOAD

A similar analysis can be carried out for the more general case described by Eqs. (3) and (4), and the details are described in the Appendix. This results in the synchronization conditions from (A22),

$$(1-\beta^2)(1-\mu_1)-\beta(2\mu_2+\alpha N)<0 . \quad (23)$$

Various limiting cases follow. When the load is purely capacitive $\mu_1=\mu_2=0$ and Eq. (22) is recovered.

When $\beta=0$, the synchronization condition is

$$1-\mu_1=1-LCI^2<0 . \quad (24)$$

In our units the condition obtained by Wiesenfeld and Swift [8] is $LC(I^2-1)>1$. For $b\ll1$, $I\gg1$ the two conditions agree.

When $\mu_1=1$, the system is in resonance and the synchronous state is always stable for $\beta>0$. Finally, when the driving current I is very large $\mu_1\gg1$, the condition becomes approximately

$$(1-\beta^2)LI+\beta(2R+1)>0 , \quad (25)$$

independent of C.

It is clear that similar calculations can be carried out for an arbitrary load impedance Z (both for one-dimensional and two-dimensional arrays), leading to well-defined conditions for synchronization or desynchronization. The growth rates of the instabilities leading to the final state are given by the coefficient of the $\sin(\theta_j-\theta_k)$ term.

ACKNOWLEDGMENT

This work was sponsored by the U.S. Department of Energy, Contract No. DE-FG02-87ER13740.

APPENDIX: *RLC* LOAD

From Eqs. (3) and (4),

$$\beta\ddot{\varphi}_k+\dot{\varphi}_k+b\sin(\varphi_k)+J=1 ,$$

$$\mu_1\dot{J}+\mu_2J+\int J\,dt=\alpha\sum_j\dot{\varphi}_j .$$

Expanding in b,

$$\varphi_k=t+\theta_k+\varphi_k^{(1)}+\varphi_k^{(2)}+\cdots , \quad (A1)$$

$$J=\bar{J}+J^{(1)}+J^{(2)}+\cdots , \quad (A2)$$

where $\varphi_k^{(n)}\sim J^{(n)}\sim b^n$. To the lowest order equations (3) and (4),

$$\beta\ddot{\theta}_k+\dot{\theta}_k+\bar{J}=0 , \quad (A3)$$

$$\mu_1\dot{\bar{J}}+\mu_2\bar{J}+\int\bar{J}\,dt=\alpha\sum_j\dot{\theta}_j \quad (A4)$$

have a solution

$$\theta_k=\text{const} \quad \bar{J}=0 . \quad (A5)$$

To the first order in b,

$$\beta\ddot{\varphi}_k^{(1)}+\dot{\varphi}_k^{(1)}+J^{(1)}=-b\sin(t+\theta_k) , \quad (A6)$$

$$\mu_1\dot{J}^{(1)}+\mu_2J^{(1)}+\int J^{(1)}dt-\alpha\sum_j\dot{\varphi}_j^{(1)}=0 . \quad (A7)$$

To second order in b,

$$\beta\ddot{\varphi}_k^{(2)}+\dot{\varphi}_k^{(2)}+J^{(2)}=-b\varphi_k^{(1)}\cos(t+\theta_k) , \quad (A8)$$

$$\mu_1\dot{J}^{(2)}+\mu_2J^{(2)}+\int J^{(2)}dt-\alpha\sum_j\dot{\varphi}_j^{(2)}=0 . \quad (A9)$$

We find the solution of (A6) and (A7) in the form

$$\varphi_k^{(1)}=A_k\sin(t)+B_k\cos(t) , \quad (A10)$$

$$J^{(1)}=C\cos(t)-D\sin(t)\ . \tag{A11}$$

Substituting (A10) and (A11) into (A6) and (A7) lead to the following linear system for coefficients:

$$\beta A_k+B_k+D=b\cos\theta_k\ , \tag{A12}$$

$$A_k-\beta B_k+C=-b\sin\theta_k\ , \tag{A13}$$

$$\alpha\sum_j B_j+(1-\mu_1)C-\mu_2 D=0\ , \tag{A14}$$

$$-\alpha\sum_j A_j+\mu_2 C+(1-\mu_1)D=0\ . \tag{A15}$$

Equations (A14) and (A15) give

$$C=[(1-\mu_1)^2+\mu_2^2]^{-1}\left[-\alpha(1-\mu_1)\sum_j B_j+\alpha\mu_2\sum_j A_j\right]\ , \tag{A16}$$

$$D=[(1-\mu_1)^2+\mu_2^2]^{-1}\left[\alpha(1-\mu_1)\sum_j A_j+\alpha\mu_2\sum_j B_i\right]\ . \tag{A17}$$

These two relations together with (A12) and (A13) after summation lead to

$$\sum_j A_j=b(\{\beta+[(1-\mu_1)^2+\mu_2^2]^{-1}\alpha N(1-\mu_1)\}^2+\{1+[(1-\mu_1)^2+\mu_2^2]^{-1}\alpha N\mu_2\}^2)^{-1}$$
$$\times\left[\{\beta+[(1-\mu_1)^2+\mu_2^2]^{1}\alpha N(1-\mu_1)\}\sum_j\cos\theta_j-\{1+[(1-\mu_1)^2+\mu_2^2]^{-1}\alpha N\mu_2\}\sum_j\sin\theta_j\right]\ , \tag{A18}$$

$$\sum_j B_j=b(\{\beta+[(1-\mu_1)^2+\mu_2^2]^{-1}\alpha N(1-\mu_1)\}^2+\{1+[(1-\mu_1)^2+\mu_2^2]^{-1}\alpha N\mu_2\}^2)^{-1}$$
$$\times\left[\{\beta+[(1-\mu_1)^2+\mu_2^2]^{-1}\alpha N(1-\mu_1)\}\sum_j\sin\theta_j+\{1+[(1-\mu_1)^2+\mu_2^2]^{-1}\alpha N\mu_2\}\sum_j\cos\theta_j\right] \tag{A19}$$

Substituting (A18) and (A19) into (A12) and (A13) gives

$$A_k=b(1+\beta^2)^{-1}(\beta\cos\theta_k-\sin\theta_k)+b\alpha(1+\beta^2)^{-1}[(1-\mu_1)^2+\mu_2^2]^{-1}$$
$$\times(\{\beta+[(1-\mu_1)^2+\mu_2^2]^{-1}\alpha N(1-\mu_1)\}^2+\{1+[(1-\mu_1)^2+\mu_2^2]^{-1}\alpha N\mu_2\}^2)^{-1}$$
$$\times\Bigg\{(-[\mu_2+\beta(1-\mu_1)]\{\beta+[(1-\mu_1)^2+\mu_2^2]^{-1}\alpha N(1-\mu_1)\}+(1-\mu_1-\beta\mu_2)\{1+[(1-\mu_1)^2+\mu_2^2]^{-1}\alpha N\mu_2\})\sum_j\cos\theta_j$$
$$+([\mu_2+\beta(1-\mu_1)]\{1+[(1-\mu_1)^2+\mu_2^2]^{-1}\alpha N\mu_2\}+(1-\mu_1-\beta\mu_2)\{\beta+[(1-\mu_1)^2+\mu_2^2]^{-1}\alpha N(1-\mu_1)\})\sum_j\sin\theta_j\Bigg\} \tag{A20}$$

$$B_k=b(1+\beta^2)^{-1}(\cos\theta_k+\beta\sin\theta_k)+b\alpha(1+\beta^2)^{-1}[(1-\mu_1)^2+\mu_2^2]^{-1}$$
$$\times(\{\beta+[(1-\mu_1)^2+\mu_2^2]^{-1}\alpha N(1-\mu_1)\}^2+\{1+[(1-\mu_1)^2+\mu_2^2]^{-1}\alpha N\mu_2\}^2)^{-1}$$
$$\times\Bigg[(-[\mu_2+\beta(1-\mu_1)]\{1+[(1-\mu_1)^2+\mu_2^2]^{-1}\alpha N\mu_2\}-(1-\mu_1-\beta\mu_2)\{\beta+[(1-\mu_1)^2+\mu_2^2]^{-1}\alpha N(1-\mu_1)\})\sum_j\cos\theta_j$$
$$+(1-\mu_1-\beta\mu_2)\{1+[(1-\mu_1)^2+\mu_2^2]^{-1}\alpha N\mu_2\}$$
$$-([\mu_2+\beta(1-\mu_1)]\{\beta+[(1-\mu_1)^2+\mu_2^2]^{-1}\alpha N(1-\mu_1)\})\sum_j\sin\theta_j\Bigg]\ . \tag{A21}$$

To the second order in b one averages over the fast time scale. The right-hand side of Eq. (A8) is

$$-\langle b\varphi_k^{(1)}\cos(t+\theta_k)\rangle=(b/2)(A_k\sin\theta_k-B_k\cos\theta_k)$$
$$=(b^2/2)(1+\beta^2)^{-1}+\alpha(b^2/2)(1+\beta^2)^{-1}[(1-\mu_1)^2+\mu_2^2]^{-1}$$
$$\times(\{\beta+[(1-\mu_1)^2+\mu_2^2]^{-1}\alpha N(1-\mu_1)\}^2+\{1+[(1-\mu_1)^2+\mu_2^2]^{-1}\alpha N\mu_2\}^2)^{-1}$$
$$\times\Bigg[[(1-\beta^2)(1-\mu_1)-\beta(2\mu_2+\alpha N)]\sum_j\sin(\theta_k-\theta_j)$$
$$+[(1-\beta^2)\mu_2+2\beta(1-\mu_1)+\alpha N]\sum_j\cos(\theta_k-\theta_j)\Bigg]\ . \tag{A22}$$

[1] K. Wan, A. K. Jain, and J. E. Lukens, Appl. Phys. Lett. **51**, 1805 (1989).

[2] S. Han, B. Bi, W. Zhang, and J. E. Lukens, Appl. Phys. Lett. **64**, 1424 (1994).

[3] M. J. Wengler, B. Guan, and E. K. Track (unpublished).

[4] K. Y. Tsang, R. E. Mirollo, S. H. Strogatz, and K. Wiesenfeld, Phys. D **48**, 102 (1991).

[5] P. Hadley, M. R. Beasley, and K. Wiesenfeld, Appl. Phys. Lett. **32**, 1619 (1988).

[6] S. Nichols and K. Wiesenfeld, Phys. Rev. E **48**, 2569 (1993).

[7] S. Watanabe and S. H. Strogatz, Phys. D **74**, 197 (1994).

[8] K. Wiesenfeld and J. W. Swift, Phys. Rev. E **51**, 1020 (1995).

[9] A. Chernikov and G. Schmidt, Phys. Rev. E **50**, 3436 (1994).

[10] A. K. Jain, K. K. Likharev, J. E. Lukens, and J. E. Sauvegau, Phys. Rep. **109**, 310 (1984).